

TECHNICAL NOTE

D-1003

AN ANALYTICAL INVESTIGATION OF THE LOADS, TEMPERATURES,
AND RANGES OBTAINED DURING THE RECOVERY OF
ROCKET BOOSTERS BY MEANS OF A PARAWING

By Howard G. Hatch, Jr., and William A. McGowan

Langley Research Center
Langley Air Force Base, Va.

NATIONAL AERONAUTICS AND SPACE ADMINISTRATION
WASHINGTON

February 1962

NATIONAL AERONAUTICS AND SPACE ADMINISTRATION

TECHNICAL NOTE D-1003

AN ANALYTICAL INVESTIGATION OF THE LOADS, TEMPERATURES,
AND RANGES OBTAINED DURING THE RECOVERY OF
ROCKET BOOSTERS BY MEANS OF A PARAWING

By Howard G. Hatch, Jr., and William A. McGowan

SUMMARY

Some of the factors affecting the feasibility of recovering the first-stage booster of large rocket vehicles by means of a parawing were investigated analytically. Two example booster trajectories were considered which represent a rather broad range of burnout conditions: booster A burned out at a Mach number of 3.2 and an altitude of 90,000 feet and booster B burned out at a Mach number of 6.7 and an altitude of 203,000 feet.

Calculation of loads and skin temperatures for a parawing deployed at apogee showed that booster A experienced tolerable loads and temperatures. Range calculations revealed that the vehicle could be returned to the launching area under zero wind conditions if the subsonic lift-drag ratio was 4 or greater and the parawing loading was about 10 pounds per square foot. Booster B experienced high loads and temperatures during descent but it was found that lift modulation could be used to reduce the loads significantly. Range calculations show that booster B was not capable of gliding back to the launch site with the recovery system investigated. From the point where the initial entry was completed booster B had about the same range capability as booster A.

INTRODUCTION

The large thrust requirements of space flight necessitate large and expensive first-stage booster rockets for the launch vehicle. A substantial saving in the cost of these flights might be realized if the booster rocket were reusable. Considerable interest exists, therefore, in exploring the feasibility of recovering the expended booster for reuse.

One method suggested would utilize a device stored on the booster itself for deployment after burnout to achieve recovery. Such a device

should probably have the following characteristics: (1) lightweight construction, (2) adaptability to storage on the booster package, (3) control of deceleration within booster design limits, (4) sufficient range for flight to an available landing area, and (5) soft-landing capability. A number of devices have been proposed for this method of booster recovery. Reference 1 is a report of an investigation of combinations of parachutes, balloons, drag brakes, retro-rockets, and rotating wings as recovery devices.

Another device of this sort which has been proposed for booster recovery is the parawing. The parawing is a lightweight flexible lifting surface (see ref. 2) that shows promise of being a satisfactory recovery device.

This paper contains results of digital- and analog-computer investigations of the recovery of a booster with a parawing deployed at apogee of the trajectory of the expended first-stage booster. The first-stage boosters of two different launch vehicles are considered in order to represent a range of burnout conditions. The first (booster A) has burnout at a Mach number of 3.2 and an altitude of 90,000 feet, whereas the second (booster B) experiences burnout at a Mach number of 6.7 and an altitude of 203,000 feet. The burnout conditions for booster A result in an apogee of the expended-booster trajectory within the usable atmosphere (where there is sufficient density to alter the vehicle flight path), whereas the apogee resulting from the burnout conditions for booster B occurs out of the usable atmosphere and entry occurs at a steep flight-path angle.

A digital-computer solution was used in a preliminary study to obtain the trajectories for the booster alone and for the booster-parawing combination with constant lift-drag ratio for a parawing deployed at apogee of the expended-booster trajectory. These studies were made to determine the range covered from launch to apogee and to obtain preliminary data on the loads and stagnation air temperatures experienced during recovery.

An analog study using lift modulation (similar to the method presented in ref. 3) was made to determine whether the peak loads indicated in the preliminary digital study could be reduced to an acceptable level. Skin temperatures along the stagnation lines of the parawing nose, shroud line, and a booster tank were calculated for laminar and turbulent flow conditions. Finally, maneuvering ranges were obtained for various turn and glide programs in order to determine the effects of bank angle, lift-drag ratio, and wing loading.

L
1
7
9
8

SYMBOLS

The English system of units is used in this study. In case conversion to metric units is desired, the following relationships apply:
 1 foot = 0.3048 meter, and 1 statute mile = 5,280 feet = 1,609.344 meters.

a_r	deceleration in direction of resultant aerodynamic force, g units
C_D	drag coefficient, D/qS
C_L	lift coefficient, L/qS
D	drag, lb
g	acceleration due to gravity, ft/sec^2
h	altitude, ft
L	lift, lb
M	Mach number
q	dynamic pressure, lb/sq ft
S	parawing area, sq ft
t_t	stagnation air temperature, $^{\circ}\text{F}$
V	velocity, ft/sec
W	weight, lb
α	angle of attack (angle between the relative wind and the keel line of the parawing), deg
γ	flight-path angle, deg
ϕ	bank angle, deg

RECOVERY PROCEDURE

The recovery procedure as visualized is depicted in figure 1, where the booster is suspended below the parawing by an array of shroud lines.

After launch, burnout, and separation the expended booster coasts to the apogee of its trajectory. In this study the parawing is deployed at apogee and as the vehicle descends it is subjected to loads and aerodynamic heating that may exceed the capabilities of the system. If the loads start to become excessive, lift modulation is used in an attempt to maintain the loads at a reasonable value. When lift modulation is used, the vehicle is maneuvered toward its landing site after the modulation process is completed. If lift modulation is not required, maneuvering toward a landing site is started immediately upon deployment of the parawing.

RECOVERY-SYSTEM CHARACTERISTICS

For this investigation, only those recovery-system specifications needed for calculation of the trajectories, loads, and skin temperatures (at the stagnation line) are given. No attempt is made to determine results for specific control systems, shroud-line riggings, and heat-protection schemes. The expended booster under consideration weighs approximately 110,000 pounds, is 90 feet in length, and has a diameter of 22 feet. For comparison with the loads computed, the transverse-load design limit of the booster is assumed to be $4g$. The parawing area is chosen to give the desired wing loading.

Aerodynamic Characteristics

Information on the aerodynamic characteristics of the parawing for supersonic flight was obtained from reference 2. The only aerodynamic coefficients needed for the two-degree-of-freedom solution used to calculate the trajectories are C_L and C_D . Mach number effects were incorporated by assuming two variations of C_L and C_D with angle of attack (see fig. 2), one for the subsonic region and one for the supersonic region. (The angle of attack is defined as the angle between the relative wind and the keel line of the parawing.) The transonic region was taken as $M = 0.8$ to $M = 1.2$, and the values of C_L and C_D were obtained in this region by linear interpolation between the subsonic and supersonic values. The data are shown for a limited angle-of-attack range because one peculiarity of the parawing is that below a certain minimum positive angle of attack objectionable characteristics, such as trailing-edge flapping, occur. The minimum positive angle has not been definitely determined; in this paper the minimum value was chosen arbitrarily as 22° . In the lift-modulation studies other minimum angles were also considered in order to determine any effect of the minimum value on the ability to decrease deceleration by means of lift modulation. The supersonic data were extrapolated in the lower angle-of-attack

region as shown by the dashed lines. The subsonic values represent data obtained in the Langley 7- by 10-Foot Tunnels Branch and the extrapolations are shown by the dashed lines. The contributions of the booster and shroud lines to the aerodynamic characteristics of the system are assumed to be small in comparison with those of the parawing and were therefore neglected in this study. Hence the aerodynamic data represent the parawing alone, and the lift-drag ratios used in the study may be optimistic on the basis of range calculations.

Materials Used for Aerodynamic-Heating Calculations

Estimates of the skin temperatures at the stagnation line that could be expected on the parawing, shroud lines, and booster tank during recovery require that certain materials and construction be assumed.

The material selected for the parawing was woven steel-fiber cloth weighing about 0.068 lb/sq ft with a thickness of 0.0017 inch and a heat capacity of 0.12 Btu/lb-°R. The inflated keel and leading edges were equal in length and each was 8 feet in diameter. The shroud lines were assumed to be steel rods 1.5 inches in diameter with a heat capacity the same as that of the parawing material. A cluster of aluminum tanks was assumed to compose the body of the booster. These were each 70 inches in diameter with a wall thickness of 0.042 inch and a heat capacity of 0.226 Btu/lb-°R.

TRAJECTORY STUDIES

Expended-Booster Trajectories

A digital-computer solution was used to obtain the trajectories of the two typical first-stage boosters after separation. Time histories of the trajectory variables are shown in figure 3. The trajectory after booster separation was calculated by means of the two-degree-of-freedom equations of motion obtained from reference 4. It was assumed that the longitudinal axis of the booster remained parallel to the velocity vector and that separation transients could be neglected. The booster drag coefficients used to calculate the trajectories were $C_D = 0.3$ for Mach numbers of 2.7 and below, and $C_D = 0.5$ for Mach numbers above 2.7. These values were averaged from unpublished flight data. The results indicate that booster A reached an altitude of approximately 32 miles at its apogee, which occurred 40.8 miles down range of the launch site with a velocity of 2,121 ft/sec. Booster B had sufficient velocity and altitude at burnout to reach an apogee of approximately 100 miles with a velocity of 6,749 ft/sec and a down-range distance of 230 miles.

These conditions (i.e., velocity, altitude, and range) represent the initial recovery conditions used for computing the return trajectories of a parawing deployed near apogee and are listed in table I for future reference. Since the parawing is not deployed until apogee it may be desirable to provide booster stabilization during the coast period from separation to apogee. However, the effect of such stabilization on apogee conditions was not considered in the trajectory calculations of figure 3.

Booster-With-Parawing Trajectories

The trajectory characteristics resulting from parawing deployment at apogee of the expended booster are shown in figure 4 for a constant L/D value of 1 and parawing loadings of 10 and 20 lb/sq ft. The peak resultant load and stagnation air temperature calculated along the trajectory of booster A are about 2g and 500° F, respectively. The load reached 10g and the peak stagnation air temperature was about 4,500° F for booster B. It is to be noted that the loads and temperatures of booster A are tolerable, whereas those experienced by booster B are excessive. In considering the load limits of the system, it is evident that one of the troublesome tasks will be to keep the transverse loads of the booster within design limits. Loading values calculated along the trajectories represent decelerations in the direction of the resultant aerodynamic force. The transverse loading experienced by the booster, in relation to the resultant loading calculated, would depend upon the angle of attack and the angle between the longitudinal axis of the booster and the parawing keel. Hence the transverse loads could be somewhat lower than the resultant decelerations shown in figure 4, depending on the rigging of the shroud lines.

These results indicated that it was desirable to investigate lift modulation to see whether the loads could be reduced and to determine the skin temperatures of components of the recovery system. It was also desirable to calculate the longitudinal and lateral range capabilities to determine whether the parawing system could return to the launch site and to determine how its range is affected by different parameters such as bank angle during the turn, L/D, and wing loading.

STUDY OF VEHICLE LOADS, TEMPERATURES, AND RANGES

In an effort to obtain further information on the loads, skin temperatures, and range capabilities of the parawing for booster recovery an analog-computer study was undertaken. Again the equations of motion used were obtained from reference 4, but with the centrifugal-force term neglected. The equations were programmed so that angle of attack

L
1
7
9
8

could be varied as a function of normal loading in order to augment the lift-modulation procedure. Skin temperatures at the stagnation line along the trajectories were calculated for both turbulent and laminar flow conditions by means of the heating equations given in references 4 and 5. Finally, it was desirable to determine the maneuvering range of the recovery system. For this the gliding and turning capabilities were programed on the analog computer so that turns were made at various bank angles to obtain the proper heading, followed by a straight gliding flight.

Load Reduction by Means of Lift Modulation

Entries with lift modulation were initiated at maximum lift (parawing angle of attack of 52°) and, during the descent, deceleration normal to the flight path was monitored. If normal deceleration exceeded a preselected value, the angle of attack was reduced as required to prevent further increase in normal deceleration. Figure 5 shows typical time histories of some of the calculated trajectory characteristics during an unmodulated and a modulated glide. It is noted that the resultant deceleration remains fairly constant during the lift-modulation period because L/D remains reasonably constant at the supersonic speeds considered. When lift modulation is used, the largest possible reduction in resultant deceleration from the unmodulated value occurs if the angle of attack is reduced so that it just reaches the given minimum angle of attack of the parawing at the time the pullout is completed. This reduction in resultant deceleration (the maximum modulation capability of the system) is displayed in figure 5 for a case in which 28° had been set as the minimum angle of attack for the modulated glide. The preselected limit on normal deceleration ($4g$) caused the angle of attack to be reduced so that it just reached 28° . The resultant maximum value of deceleration achieved during the modulated glide was about $5.6g$, as shown. If a still smaller limit on normal deceleration is chosen for the example given in figure 5, for instance $3.75g$, it will cause the angle of attack to reach the minimum value available and remain there for a time. As a consequence the resultant deceleration will peak as shown by the dashed lines in the figure. The results of this study showed that the deceleration peak rapidly increases when the limiting normal deceleration is set at a value below the optimum value.

Booster A.- Although booster A required no modulation, it is of interest to consider the decelerations that were experienced along a trajectory initiated at a velocity of 2,121 ft/sec and an altitude of 32 miles. Glides were made at constant angles of attack of 28° and 35° for parawing loadings of 10 and 20 lb/sq ft. The loads peaked twice along the trajectory, once at maximum dynamic pressure and once when L/D changed from the supersonic value of approximately 1 to the

subsonic values of either 4 or 6, depending on which angle of attack was used. The peak resultant decelerations, as listed in table II, are no greater than 2.5g.

Booster B.- Since the initial burnout conditions of booster B resulted in rather severe loads on the recovery system during entry at a constant L/D value of 1, it was decided to make a parametric study of similar trajectories to obtain general knowledge of the loads that would be experienced for trajectories of this type. Figure 6 shows the peak resultant decelerations experienced along unmodulated trajectories arbitrarily initiated at 210,000 feet with initial flight-path angles ranging from -20° to -35° and initial velocities of 6,000 ft/sec to 8,000 ft/sec. The initial conditions of booster B listed in table I and noted in figure 6 are within this range. Also shown by dashed lines are the maximum decelerations obtained by using the maximum modulation capability of the parawing for a case in which a minimum angle of attack of 28° was used. This figure shows that lift modulation can be used to reduce substantially the peak loads along the trajectory. The figure also shows that peak loads could be reduced significantly by reducing the initial velocity or flight-path angle. Thus booster trajectories with relatively low burnout velocities and flight-path angles are desirable from booster recovery considerations.

L
1
7
9
8

The effect on the peak loads of using minimum angles of attack other than 28° was determined. In order to find the extent of this effect, computer calculations were made for the same initial conditions as those given in figure 6 and an initial velocity of 8,000 ft/sec. Minimum angles of attack of 22° , 28° , 34° , and 39° were considered. Figure 7 shows the results of using the maximum modulation capability of the parawing over the angle-of-attack ranges considered. These results indicate that as long as the angle of attack could be further decreased, the loads could also be further reduced, as would be expected. The extent of the reductions ranged from 15 percent to 50 percent of the unmodulated peak loads.

Equilibrium Skin Temperatures

Skin temperatures along the stagnation lines of the parawing nose, shroud line, and booster-tank wall were calculated for laminar and turbulent flow conditions. The rate of heat flow into the material from the boundary layer was calculated by means of the empirical relations given in reference 5 for the stagnation point of blunt bodies at supersonic speeds. The relations are dependent upon the radius of curvature of the body, velocity, and atmospheric density. Booster-tank calculations were based on the dimensions of one tank of the cluster and it was assumed that the associated flow was characteristic of an isolated tank (no consideration was given to actual flow conditions about the

one tank under the influence of the other tanks). Values of constants for laminar and turbulent flow used in the equation are given in reference 5. The equations used for the net rate of heat transfer by radiation from the surface and heat absorbed by the structure are given in reference 4. The heating rate of infinite cylinders is also known to be dependent upon the cosine function of the sweep angle. The sweep angle is defined as the angle between the normal to the longitudinal axis of the body and the relative wind. Since the parawing nose approximates a spherical shape the sweep angle does not affect the skin temperature experienced at the stagnation point, but the shroud-line and booster-tank skin temperatures are predominantly affected by the sweep angle. No attempt was made to calculate the skin temperature on the ends of the booster because of the complexity of the structure. Also, no attempt was made to determine the temperature gradients through the material. Because of the choice of dimensions and materials used and the limitations of the heating equations, these calculations represent approximate temperatures for supersonic flight, and more refined temperature tests or calculations would be desirable for a specific system.

Booster A.- Calculations showed that the peak stagnation air temperature along the trajectories of booster A was about 500° F. Generally, skin temperatures along the trajectories can be expected to be no greater than the peak stagnation air temperature calculated. Hence aerodynamic heating was assumed to be tolerable and no further skin-temperature calculations were made for booster A.

Booster B.- The parametric study of loads experienced along trajectories similar to that of booster B also included a calculation of skin temperatures. The peak skin temperatures experienced during the unmodulated trajectories are shown in figure 8 for turbulent and laminar flow conditions. The shroud-line and booster temperatures shown in the figure were calculated for constant sweep angles of 22° and 38° , respectively. The temperatures shown for the booster probably represent practical maximum values because the sweep angle of 38° corresponds to a parawing angle of attack of 52° (the booster is assumed to be suspended parallel to the parawing keel line), which would be high for a practical system. The stagnation-line skin temperatures shown in figure 8 for the shroud line are probably not practical maximum values, because with an array of shroud lines one line is apt to be at 0° sweep angle and experience maximum heating at any one time.

The effect of modulation is displayed in figure 9, which is a time history of the temperatures calculated along the trajectory of booster B for an unmodulated and a modulated entry with turbulent flow conditions throughout the glide. The trajectories in this figure correspond to those represented by the time histories of figure 5. The skin temperature on the parawing for the modulated entry has shown a slight increase because of the increase in velocity and total pressure for these

trajectories. Skin temperatures of the shroud line were calculated for an initial sweep angle of 22° and increased significantly because during modulation the sweep angle went through 0° and maximum heating was experienced. The peak temperature on the booster remained about the same for the modulated case although the sweep angle increased.

One further point of interest is that if transition from laminar to turbulent flow took place during maximum dynamic pressure the parawing nose would be expected to react quickly to increases in heating rate, whereas the booster tank and shroud line have noticeable lag. (See fig. 9.) Therefore, if the flow did not stay turbulent too long the temperatures on the booster and shroud line might not reach those calculated for continuous turbulent flow, but the temperatures on the parawing nose probably would. Tests in the Langley 11-inch hypersonic tunnel have indicated that complex flows exist about a parawing configuration with shroud lines. Hence localized areas of high heating may occur, such as where the bow shock wave impinges on shroud lines. The particular areas experiencing high heating rates are too complex to be considered in this paper.

L
1
7
9
8

Range

The longitudinal and lateral range capabilities were determined by initiating a turn at a certain bank angle, holding this bank angle until a desired heading change was reached, and then instantaneously rolling back to zero bank angle and performing a straight glide at the new heading to zero altitude. All glides were made at a constant parawing angle of attack, with one exception to be noted later. Atmospheric wind velocities were not considered for these calculations.

Booster A.- Profiles of straight glides with the initial (or apogee) conditions of booster A are shown in figure 10. They were obtained by gliding at a constant angle of attack of 28° or 35° and a W/S value of 10 or 20 lb/sq ft. In the supersonic region the glide was made at $L/D \approx 1$. In the subsonic region the angle of attack of 28° corresponds to $L/D = 6$, and the angle of 35° corresponds to $L/D = 4$. The change in glide slope from the supersonic $L/D \approx 1$ to the subsonic value of 4 or 6 results in transient oscillations which can be seen in figure 10. For a given value of L/D , the configuration with lighter parawing loading had greater range than the configuration with heavier parawing loading. This result can be explained by the fact that the pullout for the configuration with the heavier parawing loading occurred at a lower altitude and more energy was lost during this maneuver than for the pullout at the lower parawing loading.

Because initiation of descent with the burnout conditions of booster A presented no great deceleration problem, lift was not

modulated and turns were initiated at apogee, the point of parawing deployment. Figure 11 shows the lateral and longitudinal ranges obtained with subsonic $L/D = 6$ (a 28° angle of attack) and bank angles of 10° , 30° , and 60° . These results indicate that the maximum range for a given heading change is a function of the bank angle.

It is noted that for small heading changes the greater ranges were obtained with a shallow bank, whereas for large heading changes the greater ranges were obtained with a larger bank angle. However, the spread in range at different bank angles for small heading changes was much smaller than that for large heading changes. Therefore a bank angle of 30° seems to be a reasonable compromise to obtain the greatest turning range in any given direction for this configuration.

It is worth noting in figure 11 that the maximum return range for booster A was roughly 70 miles. As indicated in figure 3 the vehicle was only 41 miles down range when the turn was started (apogee). Under these conditions the booster could return to the launch site (if the atmospheric winds were either nil or favorable).

Shown in figure 12 are the lateral and longitudinal ranges obtained for an angle of attack of 35° (subsonic $L/D = 4$). In this case there is a less clearcut indication of an optimum bank angle for a destination to the rear of the parawing deployment point. However, a 30° bank angle still appears to give the best results, though 60° is almost as good for 180° heading changes. In this case the range for a 180° heading change was only 40 miles so that return to the launch site is marginal.

Figure 13 shows the effects of lift-drag ratio and wing loading on the lateral and longitudinal ranges for a maneuver in which the heading change was made with a bank angle of 30° . The substantial decrease in range for the combination of low L/D and high W/S is attributed to the low altitude at which subsonic pullout was obtained and the subsequent steeper glide slope at subsonic speeds. (See fig. 10.) Figure 13 indicates that under some conditions booster A could not return to the launch area.

There is an additional point of interest in these range data. As previously stated, the resultant deceleration peaked twice, once at maximum dynamic pressure in the supersonic region and once at the pullout as a result of the change to subsonic L/D . These peaks occurred about 30 seconds apart. For straight glides and shallow banked turns the deceleration at maximum dynamic pressure in the supersonic region was greater than the deceleration at subsonic pullout. (See table II.) However, for steeply banked turns the subsonic pullout deceleration was greater than the deceleration at maximum dynamic pressure, although the resultant deceleration never exceeded $3.25g$.

Booster B.- The initial conditions of booster B produced excessive deceleration during entry, and therefore lift modulation was used. On the assumption that the maximum modulation capability was needed at the time of excessive deceleration, a controlled pullout was completed before any attempt was made to turn. After completion of the pullout two angle-of-attack programs, both for a W/S value of 10 lb/sq ft, were used in making the turns: one initiated at 52° and one at 28° .

In the first program turns were calculated by holding the angle of attack at 52° (maximum lift) until a Mach number of 1 was reached; then the angle of attack was changed linearly in 5 seconds to 28° (subsonic $L/D = 6$) and the glide was continued at that angle of attack. In the second program the turns were calculated by holding the angle of attack at 28° through the entire maneuver. The initial conditions for these programs are shown in table I. The range results of the first program are shown in figure 14 and the results of the second program in figure 15.

L
1
7
9
8

The only significant difference between the two types of turns is that the first program enabled the vehicle to increase the range for a 180° heading change by 10 miles over that for the second program. However, since the turns of figure 14 were initiated 7 miles farther down range than those in figure 15 because of the increased time required to complete the lift modulation procedure, there is little net gain. The results of figures 14 and 15 also show that from the turning point (after lift modulation), the lateral maneuvering capability of booster B is similar to that of booster A. Since booster B is 460 miles down range at the initiation of the turns, an alternate landing site is required.

There is one additional point of comparison between the range data for the turns of figure 15, which were initiated at relatively high velocity and low altitude, and for the turns in figure 11 for booster A, which were initiated at relatively low velocity and high altitude. The turns in both instances were made at a constant α of 28° and wing loading of 10 lb/sq ft; however, to realize maximum range in any given direction, in figure 15 the best compromise for bank angle was 60° whereas in figure 11 the best compromise was 30° . Thus the best compromise for constant bank angle and constant L/D in the gliding turns to achieve maximum range in any given direction is apparently a function of the initial conditions.

CONCLUDING REMARKS

Loads, skin-temperature, and range calculations were conducted for the recovery of first-stage booster rockets by means of a parawing deployed at apogee of the expended-booster trajectory. Two example boosters were considered which represent a large range of burnout

conditions: booster A burned out at a Mach number of 3.2 and an altitude of 90,000 feet, and booster B burned out at a Mach number of 6.7 and an altitude of 203,000 feet.

The recovery system for booster A experienced tolerable loads and temperatures. In addition, range calculations generally showed that if the subsonic lift-drag ratio is 4 or greater and the parawing loading is about 10 lb/sq ft, the booster could return to the launching site when zero or favorable wind conditions exist. Thus recovery from burn-out conditions of this type is feasible.

L
1
7
9
8
The burnout conditions of booster B lead to a more difficult recovery than for booster A. Loading calculations showed that lift modulation can be used to reduce significantly the peak loads, possibly to within the design limit of the booster. Studies also indicate that parawing rigging may aid in maintaining low transverse loads on the booster. Temperatures can become high if turbulent flow conditions exist during maximum heating. Also, the temperature of the booster and shrouds can be affected by lift modulation because of changes in sweep angle, but the parawing-nose temperature is only slightly altered. Range calculations showed that the recovery system investigated would require a landing site different from the launch site.

Langley Research Center,
National Aeronautics and Space Administration,
Langley Air Force Base, Va., October 17, 1961.

REFERENCES

1. Lysdale, C. A.: Launch-Vehicle Recovery Techniques. Paper No. 61-51, Inst. Aerospace Sci., Jan. 1961.
2. Rogallo, Francis M., Lowry, John G., Croom, Delwin R., and Taylor, Robert T.: Preliminary Investigation of a Paraglider. NASA TN D-443, 1960.
3. Grant, Frederick C.: Modulated Entry. NASA TN D-452, 1960.
4. Eggleston, John M., and Young, John W.: Trajectory Control for Vehicles Entering the Earth's Atmosphere at Small Flight-Path Angles. NASA TR R-89, 1961. (Supersedes NASA MEMO 1-19-59L.)
5. Chapman, Dean R.: An Analysis of the Corridor and Guidance Requirements for Supercircular Entry Into Planetary Atmospheres. NASA TR R-55, 1960.

L
1
7
9
8

TABLE I.- PERTINENT INITIAL RECOVERY CONDITIONS

Booster	Remarks	h, ft	V, ft/sec	γ , deg	Distance from launch site, miles
A	Near-apogee conditions of expended booster - parawing deployed and turns initiated at this point.	168,242	2,121	-3.1	40.8
B	Near-apogee conditions of expended booster - parawing deployed at this point.	532,910	6,749	0.4	230.0
B	Convenient conditions for initiation of analog-computer program.	244,554	7,951	-30.7	410.6
B	Initial conditions for turns made at angle of attack of 28° . (Lift modulation completed.)	116,500	4,256	-4.7	461.7
B	Initial conditions for turns made at angle of attack of 52° . (Lift modulation completed.)	117,500	3,160	10.3	468.7

L
1
7
9
8

TABLE II.- PEAK LOADS EXPERIENCED ALONG BOOSTER A TRAJECTORIES

[Unmodulated lift]

L/D (subsonic)	W/S, lb/sq ft	Peak a_r at maximum q, g units	Peak a_r during subsonic pullout, g units
6	20	2.50	1.56
4	20	2.22	1.56
6	10	2.17	1.56
4	10	1.88	1.56

L
1
7
9
8

L-1798

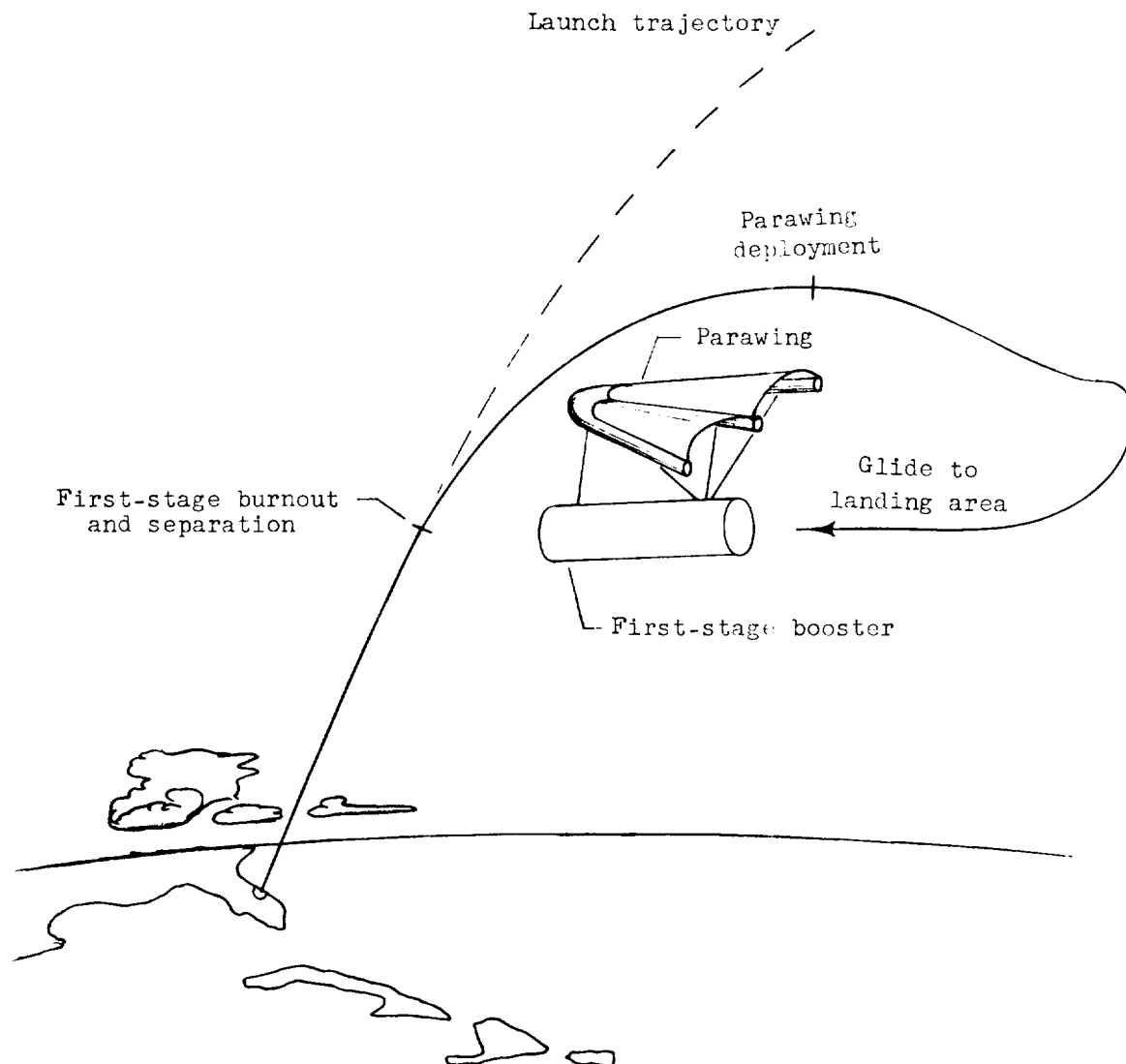
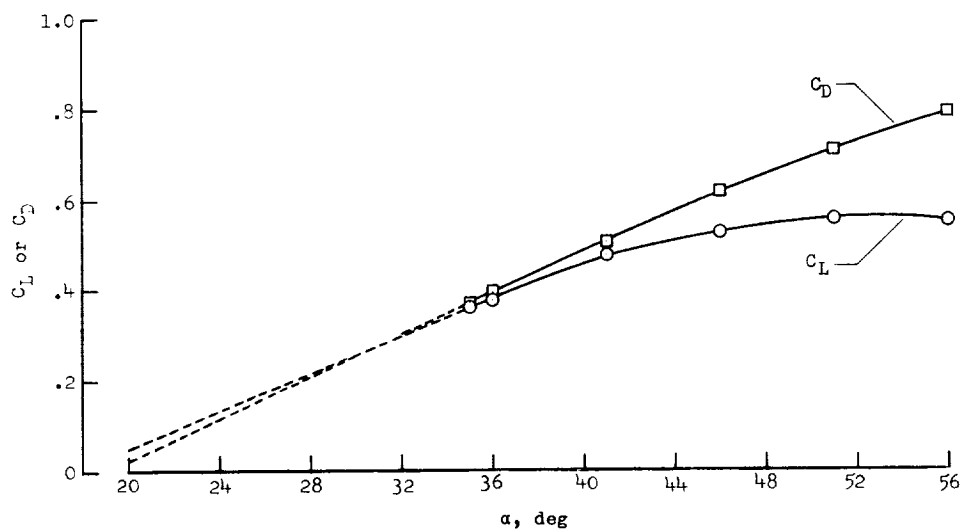
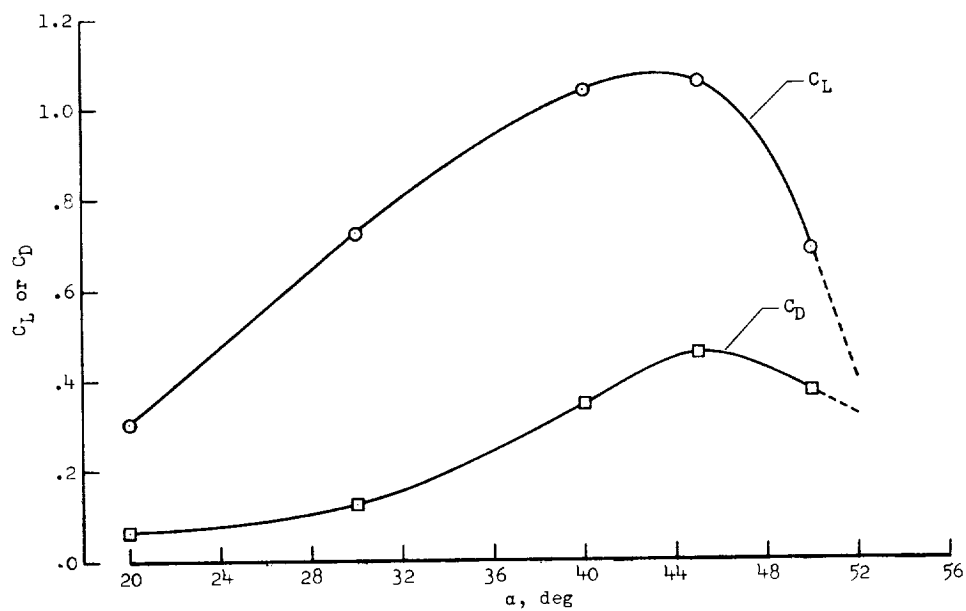


Figure 1.- Schematic sketch of recovery procedure.



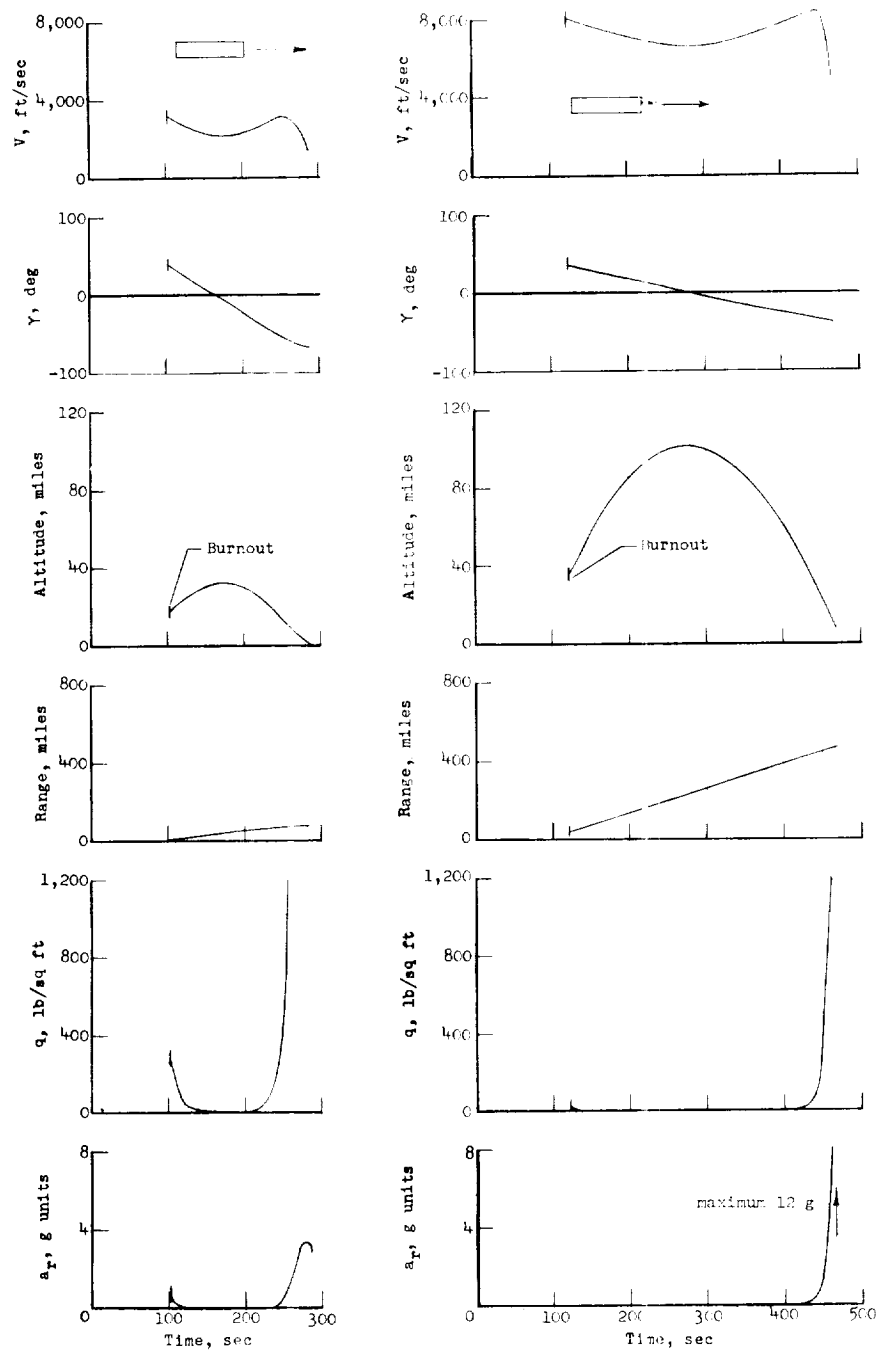
(a) Supersonic.



(b) Subsonic.

Figure 2.- Lift-drag characteristics of a parawing.

L-1798



(a) Booster A.

(b) Booster B.

Figure 3.- Typical trajectory characteristics for first-stage booster alone after burnout and separation from other stages.

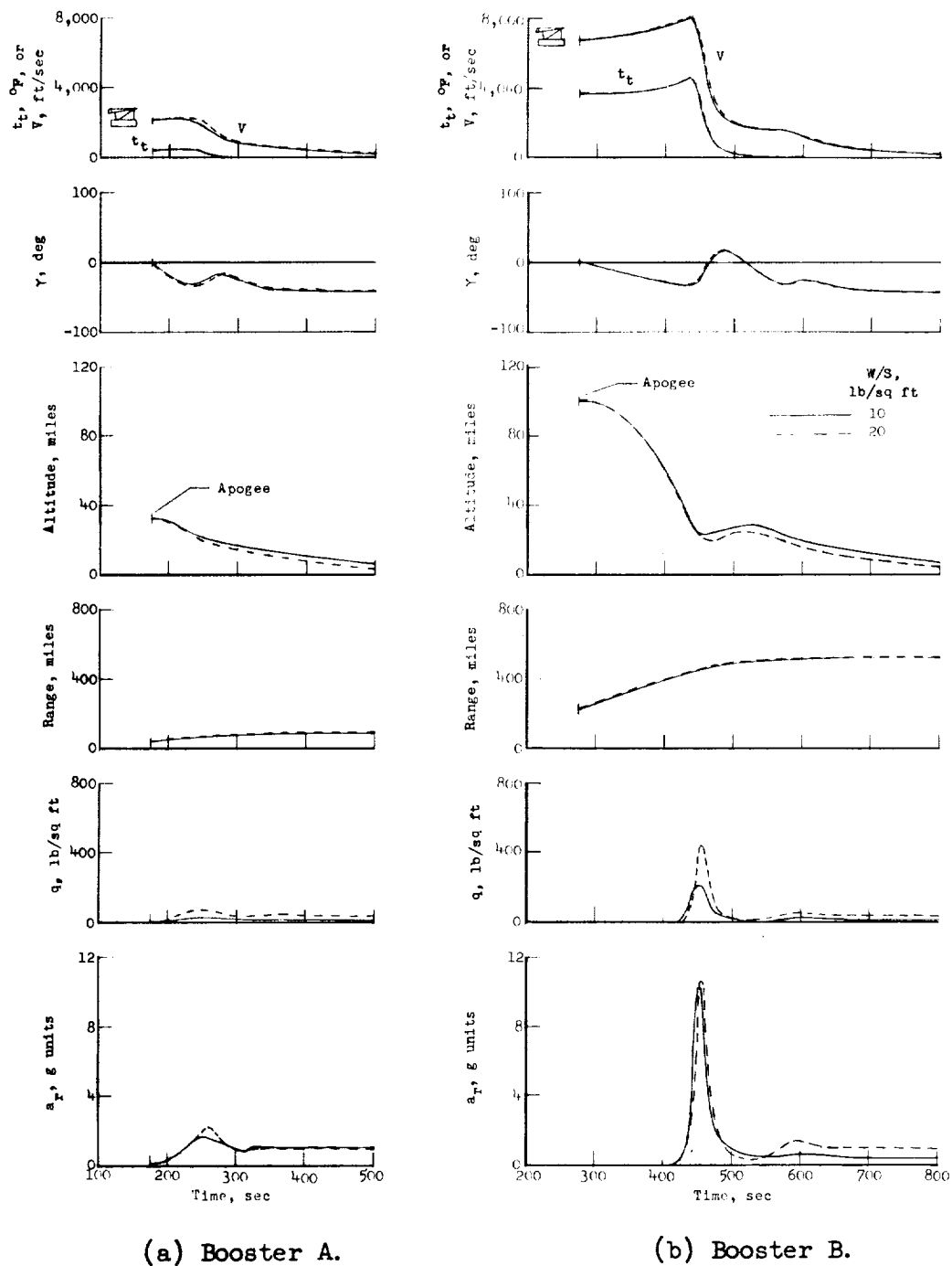
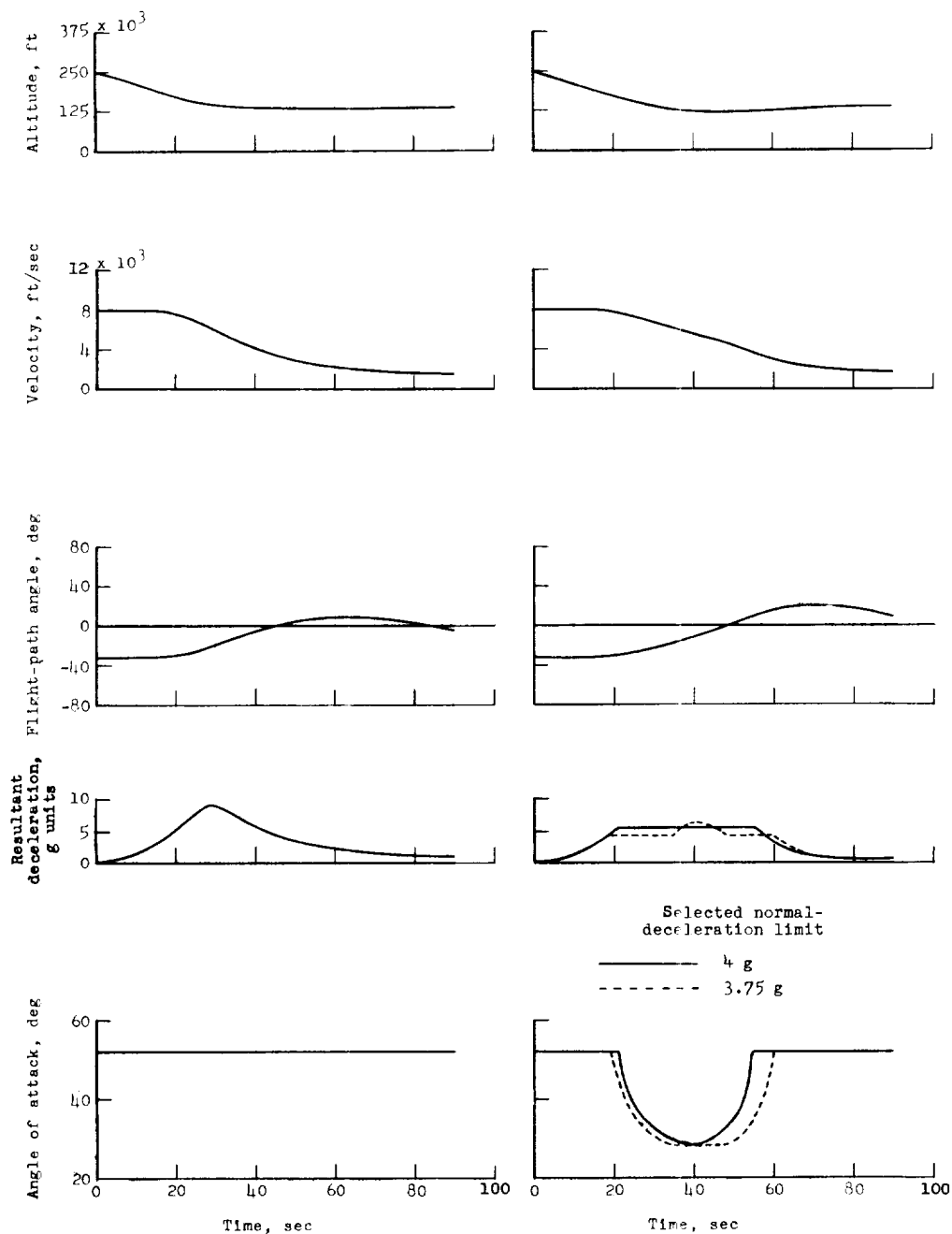


Figure 4.- Trajectory characteristics of recovery system after parawing deployment at apogee of typical first-stage-booster trajectories. Constant $L/D = 1.0$; $C_L = 0.34$.



(a) Unmodulated.

(b) Modulated.

Figure 5.- Typical time histories of an unmodulated and a modulated entry for booster B initial conditions (see table I).
 $W/S = 10 \text{ lb/sq ft}$.

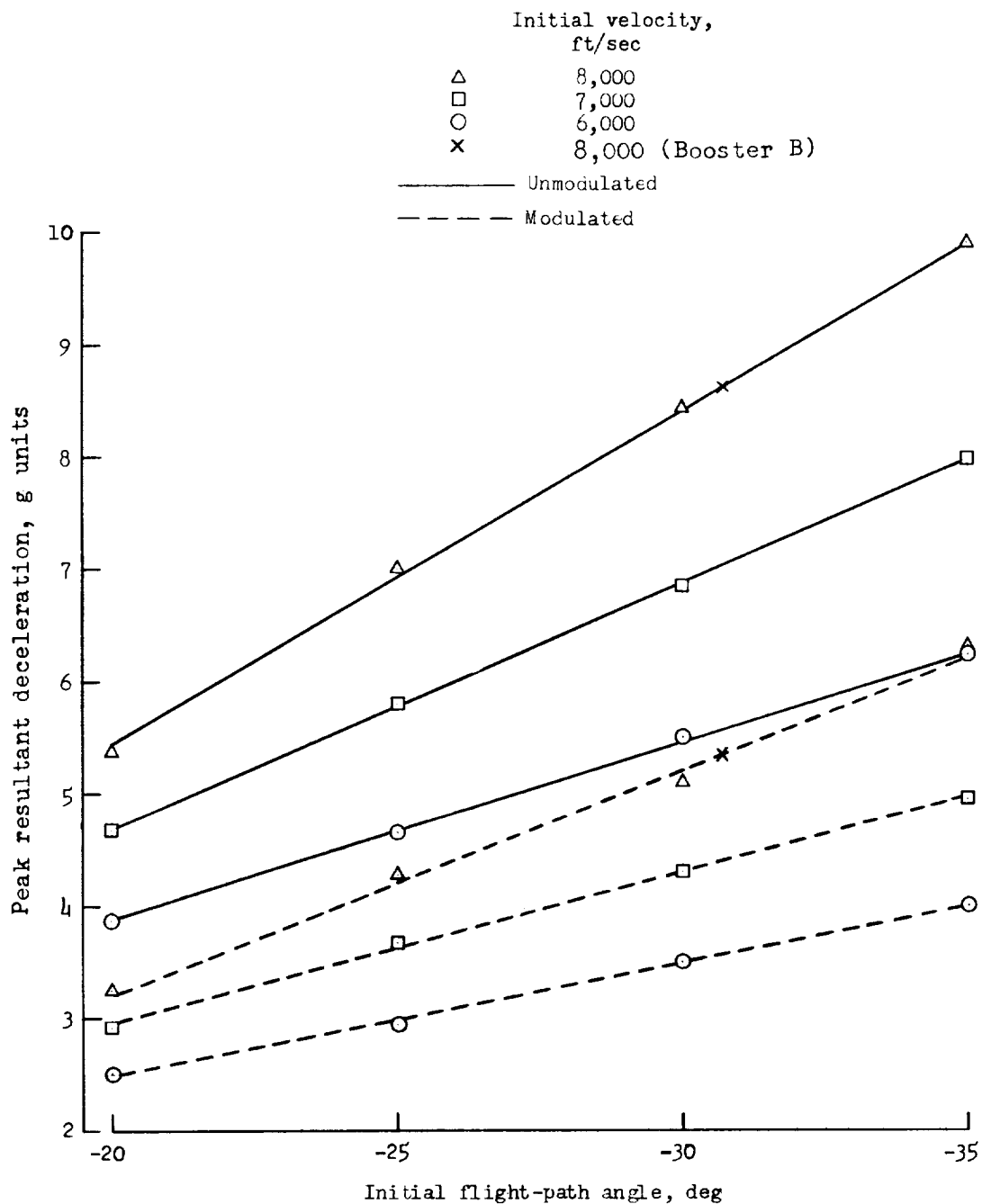


Figure 6.- Peak resultant decelerations for unmodulated glides and maximum resultant decelerations obtained by use of maximum modulation capability. Initial altitude was 210,000 feet and angle-of-attack range was 28° to 52° .

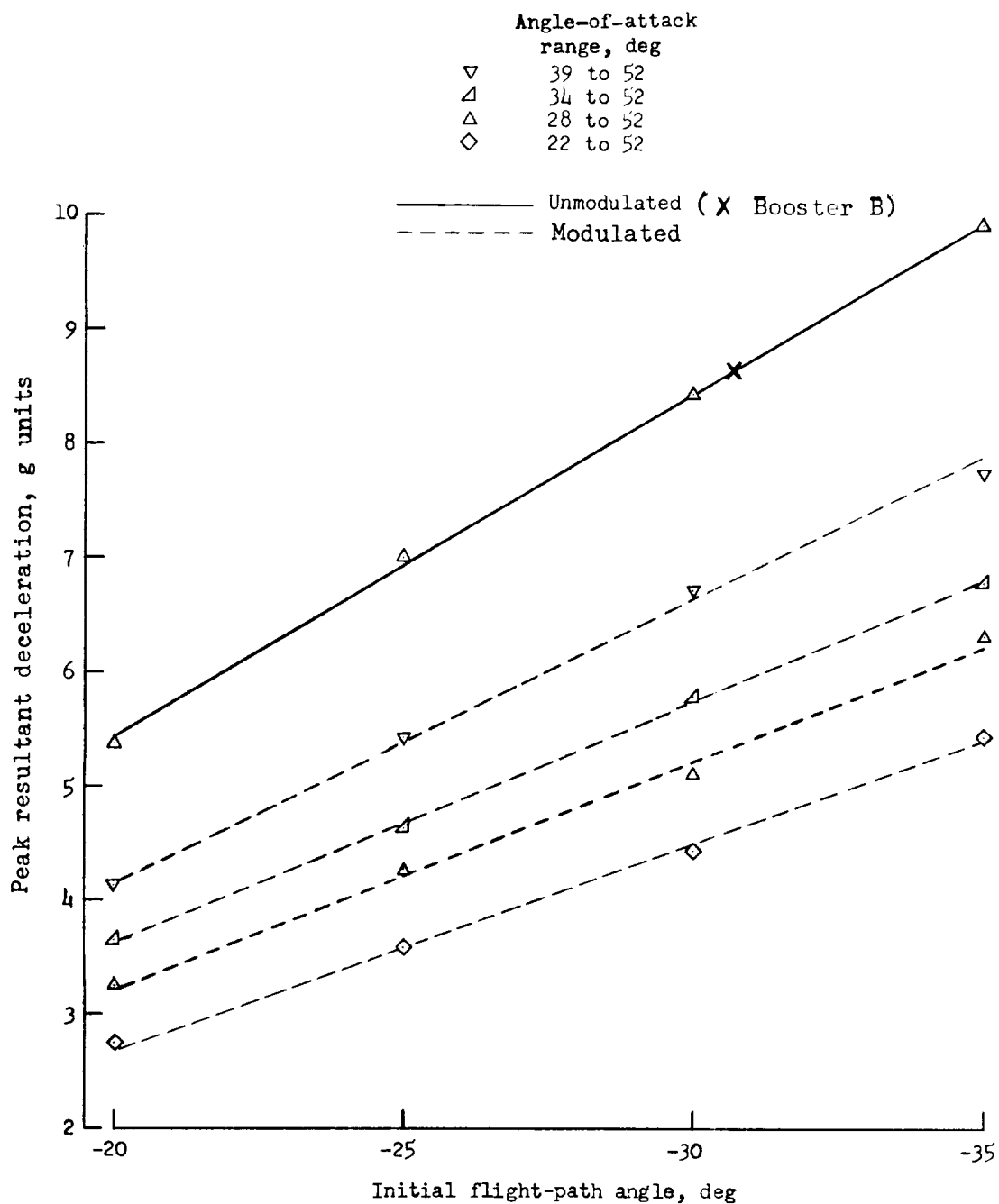


Figure 7.- Peak resultant deceleration for unmodulated glide and maximum resultant deceleration obtained by use of maximum modulation capability for several minimum angles of attack. Initial altitude was 210,000 feet and initial velocity was 8,000 ft/sec.

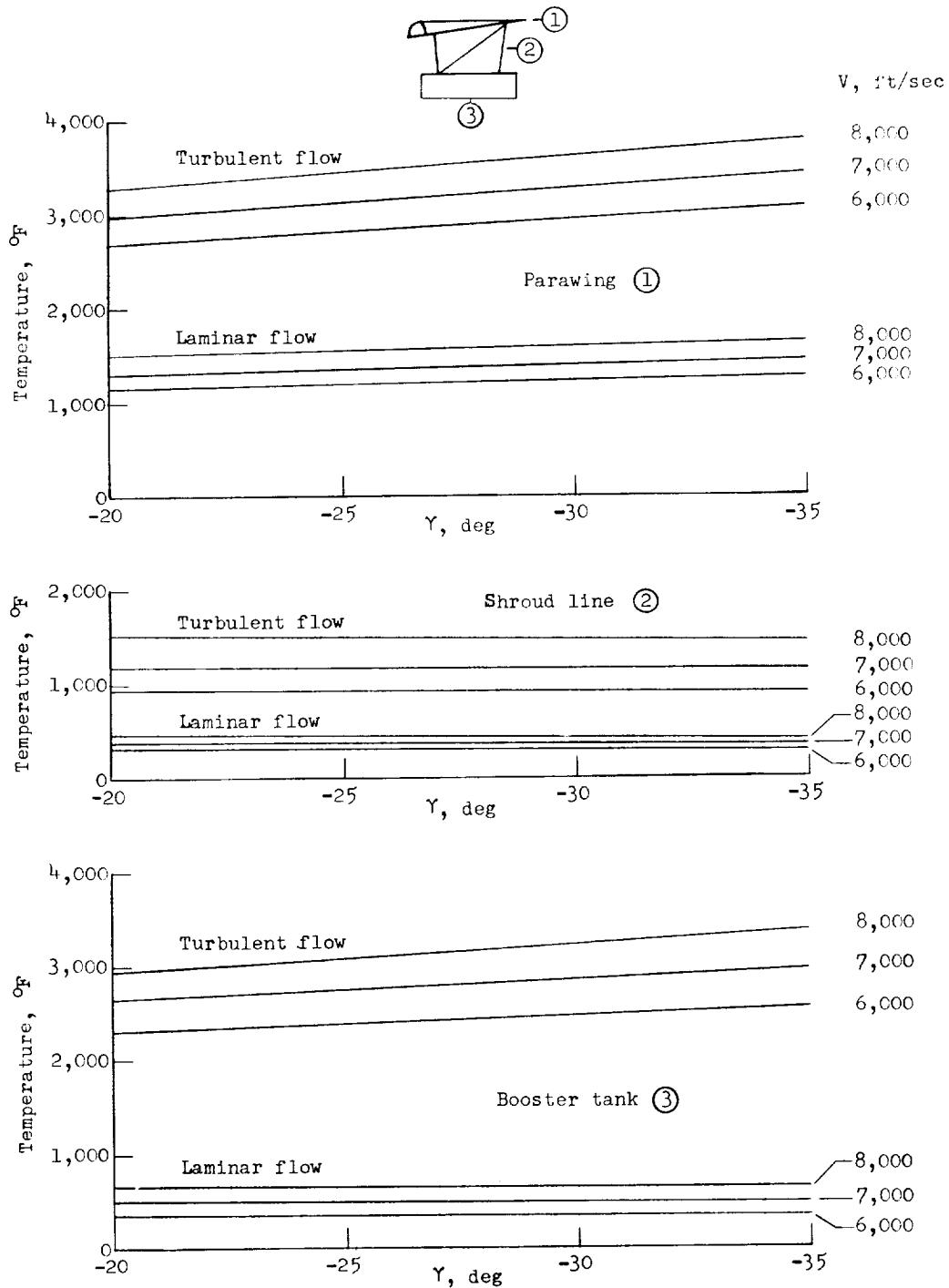
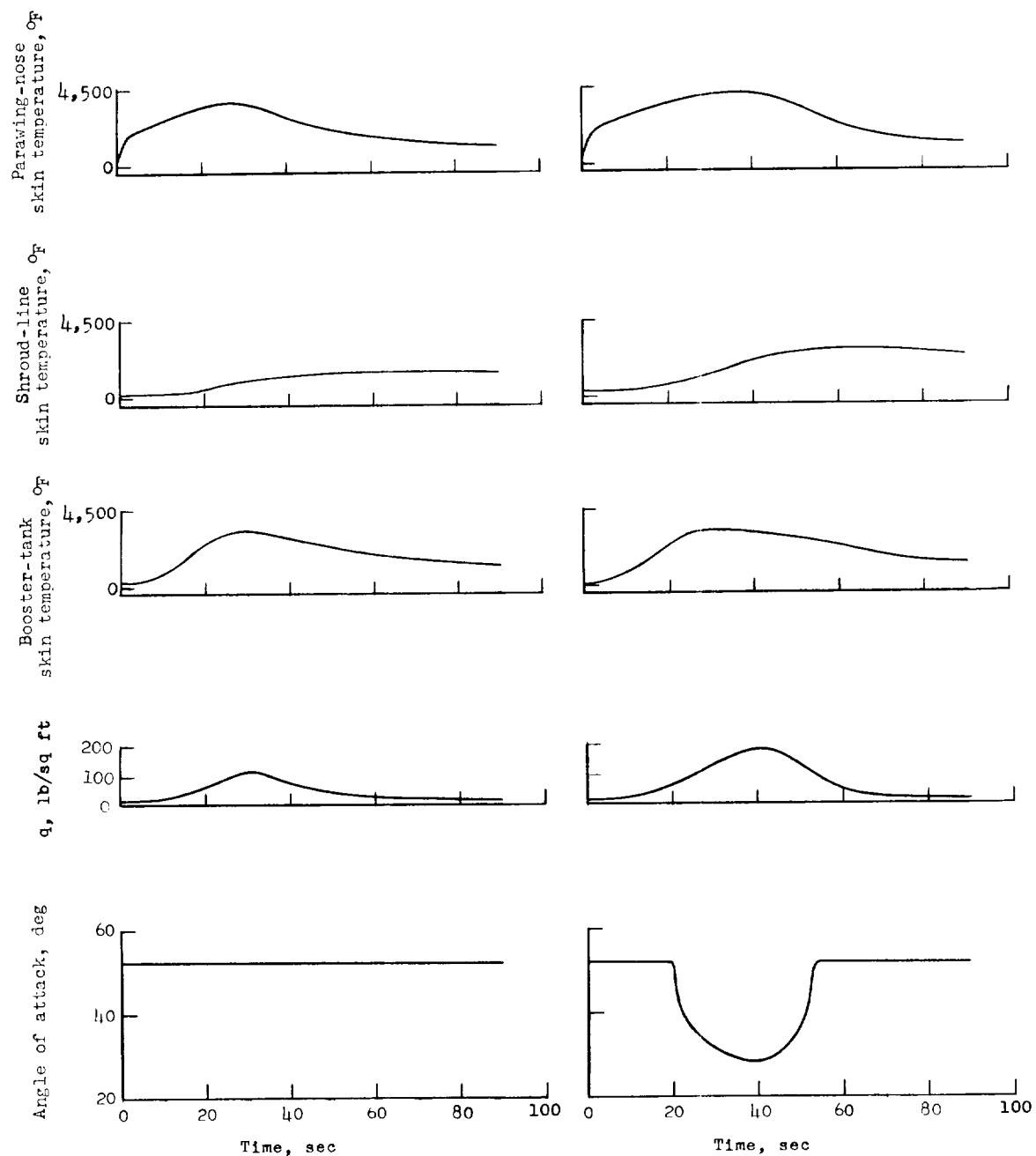


Figure 8.- Peak skin temperature along unmodulated trajectories initiated at altitude of 210,000 feet for several entry velocities and flight-path angles. $W/S = 10 \text{ lb/sq ft}$.

L-1798



(a) Unmodulated.

(b) Modulated.

Figure 9.- Typical time histories of skin temperatures for turbulent flow along an unmodulated and a modulated entry trajectory for booster B initial conditions (see table I).

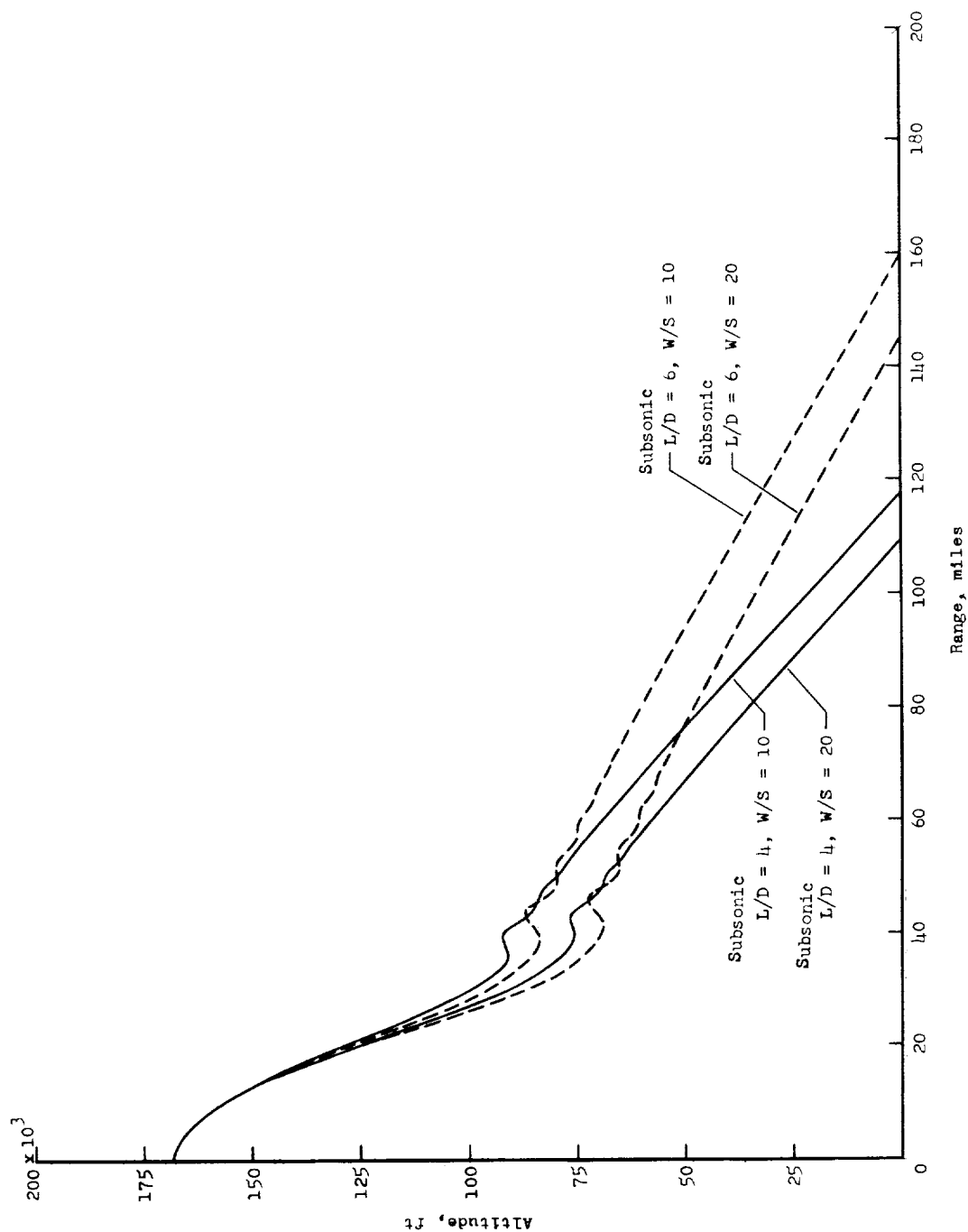


Figure 10.- Profile of straight glide for booster A initial conditions.

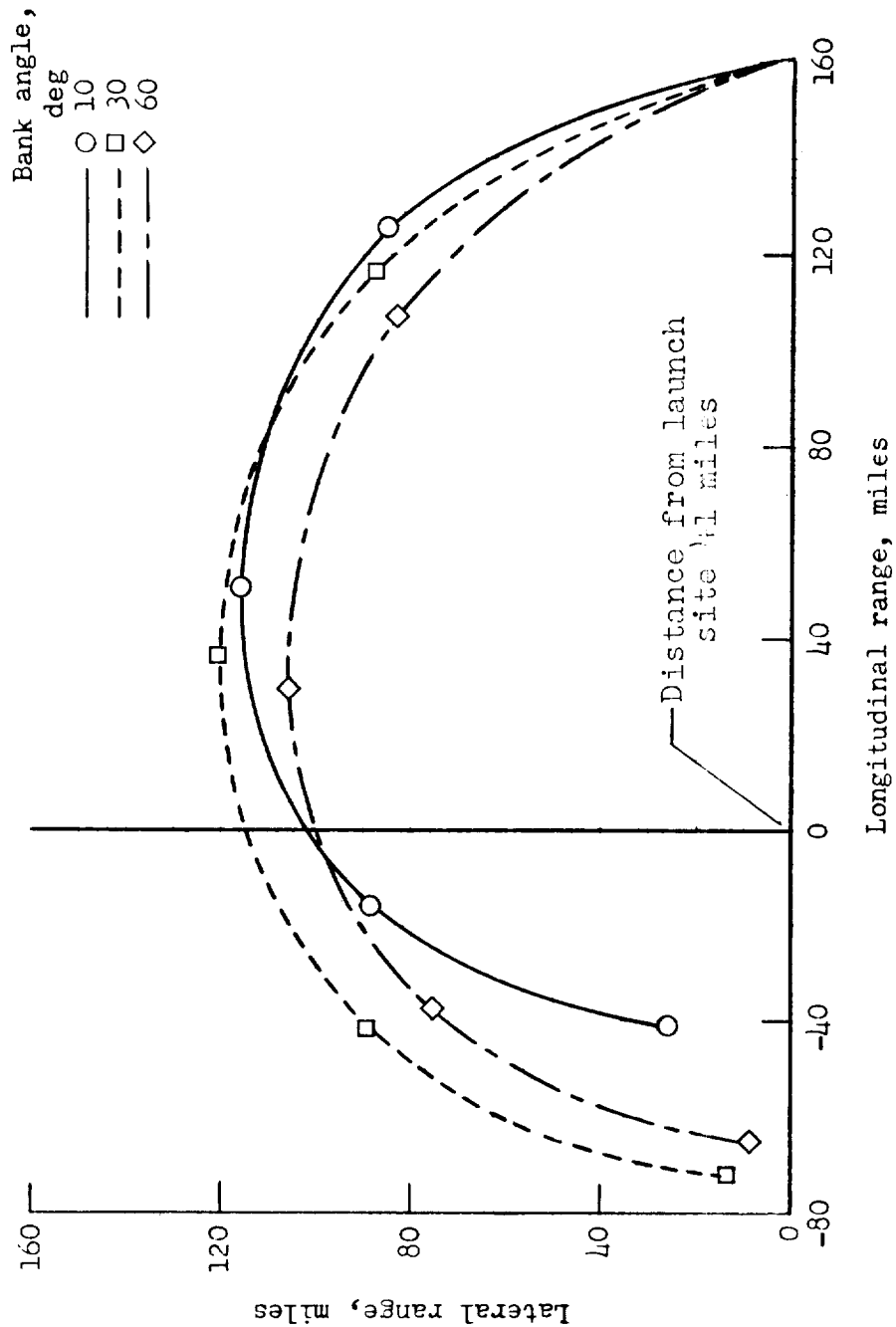


Figure 11.- Ranges obtained for booster A initial conditions and the α value for subsonic $L/D = 6$. $W/S = 10 \text{ lb/sq ft}$.

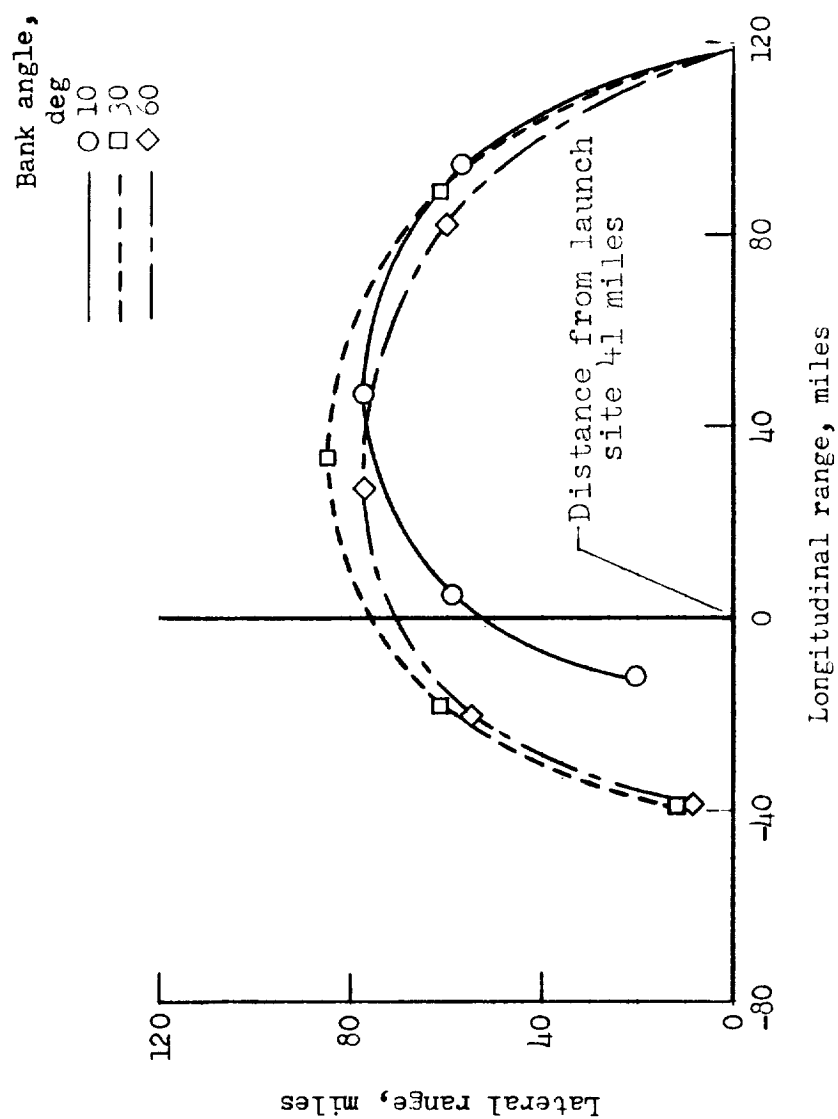


Figure 12.- Ranges obtained for booster A initial conditions and the α value for subsonic $L/D = 4$. $W/S = 10 \text{ lb/sq ft}$.

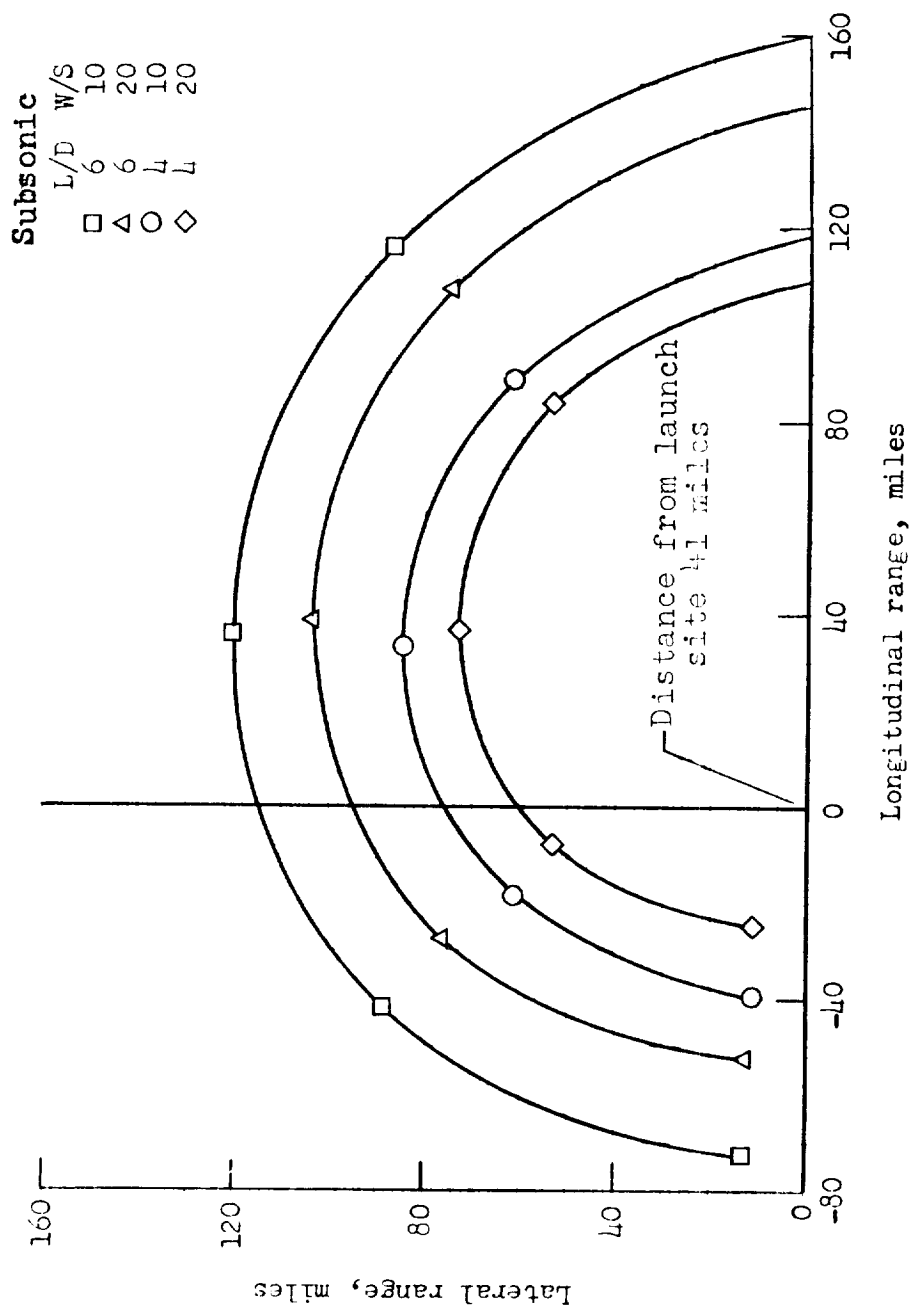


Figure 13.- Ranges obtained for booster A initial conditions. $\phi = 30^\circ$.

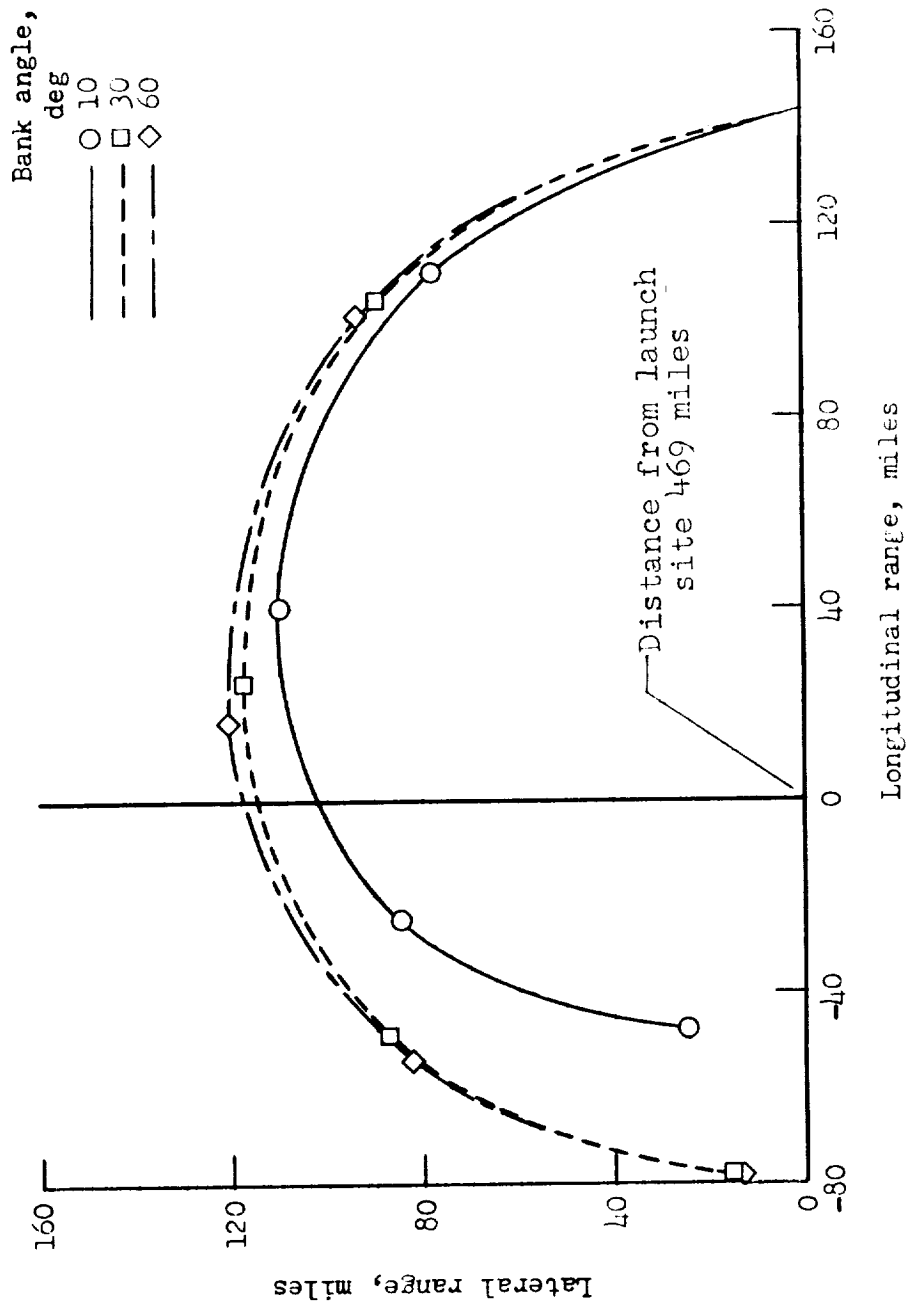


Figure 14.- Ranges for booster B initial conditions after lift modulation. Turn initiated at maximum lift for supersonic flight and changed to $L/D = 6$ for subsonic flight.
 $W/S = 10 \text{ lb/sq ft.}$

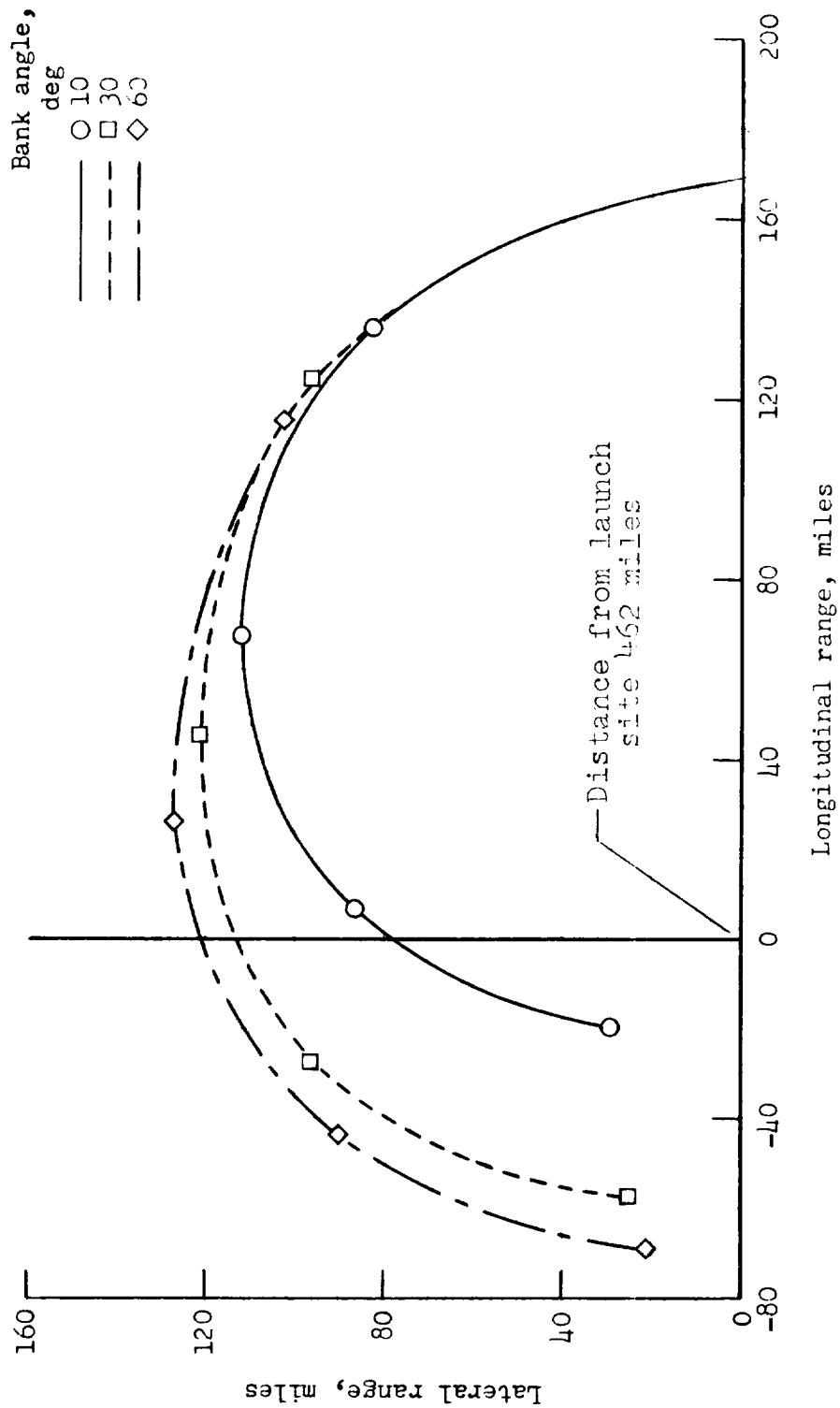


Figure 15.- Ranges for booster B initial conditions after lift modulation. Turns made at the α value for subsonic $L/D = 6$. $W/S = 10$ lb/sq ft.

